Dyes and Pigments 139 (2017) 65–72

Contents lists available at ScienceDirect

Dyes and Pigments

journal homepage: www.elsevier.com/locate/dyepig

Non-covalent complexes of polycationic fullerene C_{60} derivative with xanthene dyes – Spectral and photochemical properties in water and in liposomes

Alexandra Yu. Belik [a], Alexander Yu. Rybkin [a, *], Ilya I. Voronov [a], Nikolay S. Goryachev [a], Dmytro Volyniuk [b], Juozas V. Grazulevicius [b], Pavel A. Troshin [c, a], Alexander I. Kotelnikov [a, **]

[a] Institute of Problems of Chemical Physics, Russian Academy of Sciences, Chernogolovka, Moscow region, 142432, Russia
[b] Department of Polymer Chemistry and Technology, Kaunas University of Technology, Radvilenu pl. 19, LT-50254, Kaunas, Lithuania
[c] Skolkovo Institute of Science and Technology, Nobel St. 3, Moscow, 143025, Russia

ARTICLE INFO

Article history:
Received 1 August 2016
Received in revised form
3 November 2016
Accepted 18 November 2016
Available online 19 November 2016

Keywords:
Fullerene
Photosensitizer
Dyad
Xanthene
Water-soluble fullerene derivative

ABSTRACT

By the use of absorption spectroscopy, steady-state and time resolved fluorimetry xanthene dyes fluorescein, eosin Y and erythrosin B were shown to form complexes with polycationic fullerene derivative due to electrostatic interactions in aqueous solution and in the structure of the liposomes. It was found that the singlet excited states of dyes are effectively quenched either due to excitation energy transfer or electron transfer from singlet excited state of the dye to the fullerene core. Photodynamic activity of the complex is much higher than the activity of the dye or the fullerene derivative as the individual compounds. Photostability of the dyes increases in the complex structure as well. These effects allow predicting the development of a new generation hybrid photosensitizers. Noteworthy, one can use a dye excited only in a singlet state in combination with fullerene, which greatly enhances the directional design of such hybrid structures.

1. Introduction

Different methods of therapy, based on photodynamic action of dyes on tumors, cells and bacteria, are used at present [1–3]. Photodynamic action of dyes (usually porphyrins, chlorines and phthalocyanines) is based on their ability to go to the long-lived triplet state after photoexcitation. Then energy or electron transfer from triplet exited dye to oxygen molecule leads to generation of reactive oxygen species (ROS), which destroy biological structures.

Designing of new photosensitizers with high triplet quantum yield is an issue of the day not only for photodynamic therapy. Triplet photosensitizers have very broad application in photovoltaics [4–6], photopolymerization [7], photocatalysis [8], as luminescent molecular probes [9–11] and in the triplet-triplet annihilation photon upconversion [8,12].

According to requirements of photodynamic therapy photosensitizers also must have solubility in water, high absorption in the red light region, ability to selectively accumulate in tumor and to be quickly excreted from the body [1,13]. Because of such contradictory requirements the choice of the dye for practical use in medicine is very limited.

In the last two decades fullerenes and their derivatives attracted considerable attention as potential photodynamic drugs. Under photoexcitation they go to the triplet state with a probability close to unity, and, depending on the polarity of the medium, effectively generate singlet oxygen $^1O_2$ or superoxide anion radicals $O_2^{\bullet -}$ and other active radicals [14–16]. There are a considerable number of publications on the photodynamic effect of fullerenes and their derivatives, resulting in DNA, proteins and membranes damage, killing or slowing growth of tumor cells, viruses and bacteria [17–27]. Unfortunately, the application of fullerenes and their derivatives for photodynamic therapy in clinical practice is strongly limited by a weak absorption of fullerenes in the visible (VIS) and near infrared (NIR) spectral ranges. The short wavelength

* Corresponding author.
** Corresponding author.
E-mail addresses: alexrybkin@gmail.com (A.Yu. Rybkin), kotel@icp.ac.ru (A.I. Kotelnikov).

http://dx.doi.org/10.1016/j.dyepig.2016.11.025
0143-7208/

absorptions characteristics of fullerenes are hardly suitable for a photodynamic therapy since such beams do not penetrate deep into living tissues.

The efficiency of the photodynamic action of fullerenes can be greatly enhanced by using hybrid nanostructures (HNS) composed of fullerene derivatives bearing appended dye molecules absorbing the light in the VIS and NIR spectral ranges.

The energy redistribution in photoexcited dye–fullerene system may occur via different pathways:

1) the excitation energy can be transferred from the dye molecule to the fullerene core or vice versa depending on the energy levels of these subunits by FRET pathway, for example [28–32]. Moreover, the energy transfer to an intermediate charge transfer state (CT state) also becomes possible if such a CT state is formed in the system [33,34].
2) a photoinduced electron transfer (PET) can occur from the photoexcited dye to fullerene thus producing a charge separated state (CS state) [32,35–38]. Alternatively, the CS state can be produced via electron abstraction by the excited fullerene unit from the dye unit in the ground state.

The formation of the excited fullerene states or the fullerene radical anion in biological systems initiates a cascade of chemical reactions producing active molecular and radical species. The singlet oxygen $^1O_2$ or oxygen radical anion $O_2^{\bullet -}$ are the most common examples. The final effect of such processes is the formation of some active species under the light excitation inducing local destruction of the tissue.

The design of HNS with optimized structural, photophysical and redox parameters is a big challenge in the field of photodynamic therapy.

There are publications that describe the study of fullerene complexes with dyes, which are soluble in organic solvents [39–41]. Such structures are mainly synthesized in order to create organic photovoltaic systems [28,42–46]. It was found that the fullerene effectively quenched singlet state of dyes in non-polar solvents [29,47,48], which may lead to the efficient generation of reactive oxygen species. In some cases, the results of the photodynamic action of such hybrid structures on biological structures DNA or cells were studied [49–53]. However, in most cases, such hybrid structures are insoluble in water. There are only limited publications describing investigations of photodynamic action of water soluble fullerene-dye structures [54–59].

In this paper, we report the results of studying of the photophysical properties and photodynamic activity of HNSs based on the complexes of xanthene dyes (XD) fluorescein, eosin Y and erythrosin B with water soluble polycationic fullerene C_{60} derivative (PFD) (Fig. 1). This PFD has high water solubility (more than 100 mg/ml) due to five positive charges on addends [60]. It is well known that at neutral pH these xanthene dyes form anions or dianions in aqueous solution [61,62]. It is natural to assume that oppositely charged XD and PFD molecules may form complexes in the solution.

Fluorescein, eosin Y and erythrosin B have singlet excited levels in the range of 18300–19500 cm^{-1} and triplet levels in the range of 15150–15900 cm^{-1}, which is significantly higher in comparison to singlet and triplet levels of fullerene core (16000 cm^{-1} and 12700 cm^{-1}, correspondently [63–65]). As was mentioned above, in this case in complexes XD-PFD the effective transfer of the excitation or electron from the XD to the fullerene core can take place after photoexcitation of the dye. Further transfer of excitation or electron to molecular O_2 will lead to the generation of $^1O_2$ or $O_2^{\bullet -}$.

Thus, one can expect the effective generation of the reactive oxygen species by the fullerene during the excitation of such HNS by light in the absorption band of the dye.

Since singlet and triplet quantum yields for fluorescein, eosin Y and erythrosin B are distinguish considerably (Table 1) [7,62,66,67], it seems interesting to conduct a comparative study of the photophysical parameters and photodynamic activity of these XD-PFD complexes.

This article is devoted to the study of the regularities of the formation of XD-PFD complexes in aqueous solutions and in the structure of the liposomes, a comparative study of their photophysical properties and photodynamic activity.

2. Experimental

2.1. Reagents

The following reagents were used in the studies: fluorescein, eosin Y and erythrosin B (Sigma), NADH (nicotinamide adenine dinucleotide, Sigma), NBT (nitro blue tetrazolium chloride, Sigma), EDTA (ethylenediamine-tetraacetic acid, Sigma), Tris base (Sigma). The PFD was synthesized according to the previously reported procedures [60]. Such PFD have solubility in water greater than 100 mg/ml. The structure of the fullerene derivative was proved by the methods of IR and UV spectroscopy, ^1H and ^{13}C nuclear magnetic resonance spectroscopy, and electrospray mass spectrometry.

2.2. Photophysical and photochemical studies

Absorption spectra were recorded on Specord M40 spectrophotometer equipped with temperature-controlled cuvette section. Fluorescence steady-state spectra and fluorescence quantum yield of the dyes under study were recorded by FLS980 spectrometer (Edinburgh Instruments) and by Cary-Eclipse fluorescence

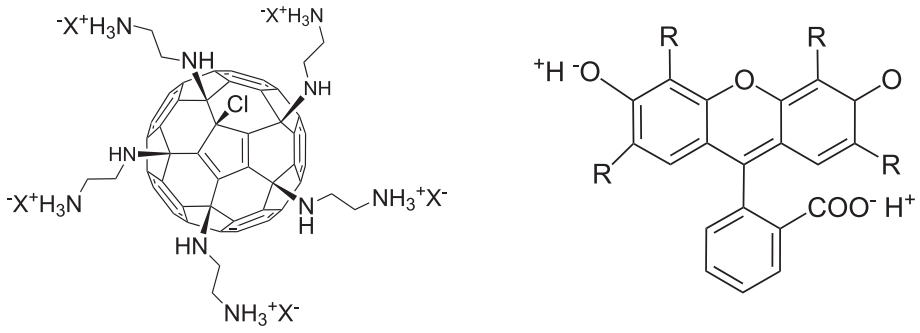

Fig. 1. PFD: X = CF_3COO^-. Xanthene dyes: R = H fluorescein; R = Br eosin Y; R = I erythrosin B.

Table 1
A comparison of photophysical properties of xanthene dyes.

	Fluorescein	Eosin Y	Erythrosin B
Fluorescence lifetime in water, ns	3.6 ± 0.2	1.04 ± 0.01	–
Fluorescence lifetime in water, ns	4.06 [62]	0.9 [69]	0.089 [70]
Shtern-Volmer constant in water, 10^5 M^{-1}	2.4 ± 0.1	3.3 ± 0.1	5.3 ± 0.2
Shtern-Volmer constant in liposomes, 10^5 M^{-1}	3.28 ± 0.05	0.52 ± 0.02	0.09 ± 0.02
The distance R_0, Å	38.0	34.4	20.0
Triplet quantum yield	0.03 [67]	0.32 [71]	0.97 [7]
Singlet quantum yield	0.93 [62]	0.68 [71]	0.03 [7]
Enhancing coefficient (E_c) of photochemical activity for XD-PFD complex in water	10.4 ± 0.2	3.2 ± 0.1	1.6 ± 0.1
Enhancing coefficient (E_c) of photochemical activity for XD-PFD complex in liposomes	1.1 ± 0.1	1.4 ± 0.1	1.3 ± 0.1

spectrophotometer. The kinetics of the fluorescence decay of xanthene dyes were recorded on a 16-channel PML-Spec detector with the use of a time-correlated SPC-530 photon counter (Becker & Hickl GmbH) with a time resolution of 2.4 ps. The sample was excited with a picosecond LDH-P-C-470 laser (PicoQuant GmbH) ($\lambda = 470$ nm, $\tau_{1/2} \leq 300$ ps, E = 1 mW). The fluorescence lifetime was calculated from the exponential approximation in the maximum of the radiation spectrum.

Phosphatidylcholine liposomes were prepared as described in Ref. [68], lipid concentration in cuvette was 10^{-4} M. The photochemical activity (relative amount of the superoxide radicals produced) of compounds PFD, XD and the XD-PFD complexes were estimated from the generation of $O_2^{\bullet -}$ using a standard formazan assay by measuring the evolution of the optical density at 560 nm as described [16]. The photochemical reaction was performed in a 10 × 10 mm quartz cuvette in a temperature-controlled cell at 20 °C. There were 2 ml of water solution (pH 6.5) which contained NADH ($4 \cdot 10^{-4}$ M), NBT ($4.8 \cdot 10^{-5}$ M), EDTA ($2 \cdot 10^{-5}$ M), the PFD compound, and/or XD in a concentration of $2 \cdot 10^{-6}$ M in the cuvette.

The cuvette was lighted with a xenon 150 W lamp through a system of optical filters selecting the 450–550 nm band (Fig. 2, curve 5). The power of the light illuminating the sample was 4.4 mW cm^{-2}.

3. Results and discussion

3.1. Analysis of photophysical effects at the interaction of PFD with xanthene dyes in water solution and in the liposomes structure

The photophysical properties of the XD-PFD complexes, which are formed by introduction into an aqueous solution PFD and XD, have been investigated. PFD at neutral pH have five positive charges and xanthene dyes fluorescein, eosin Y, erythrosin B under these conditions have one or two negative charges [61,62].

Absorption spectra, spectra of steady-state fluorescence and fluorescence decay kinetics of XD were recorded in the sequential administration of increasing concentrations of the PFD in the range of $10^{-7} - 10^{-4}$ M into the cuvette (Figs. 2–5).

Fig. 2 shows the absorption spectra of the PFD, fluorescein, eosin Y, erythrosin B as well as the transmission spectrum of the optical filters used for excitation of the sample in the study of photodynamic action of compounds. When PFD was administered in increasing concentrations in the range of $5 \cdot 10^{-7} - 2 \cdot 10^{-6}$ M there was a shift of the absorption spectrum of the dye to the red region with a substantial reduction of its absorption, as exemplified for eosin Y (Fig. 2). Simultaneously intensive stationary fluorescence decreased until complete quenching, and it was observed without changing of the decay kinetics of fluorescence (Figs. 4–5). These experimental facts suggest that the formation of static complexes XD-PFD take place in the solutions. The shift of the absorption spectra of XDs in the structure of the complexes in the red region indicates the effective interaction of electron π-orbitals of the dye and the fullerene core, and the steady-state fluorescence quenching – the effective transfer of excitation or electron from the excited singlet state of the dye to the fullerene. At the same time the fluorescence intensity and the fluorescence decay time of the free XD molecules outside the complex remain unchanged. Analysis of data on the quenching of XD steady-state fluorescence in the presence of PFD in the Stern-Volmer coordinates (Fig. 6) allows

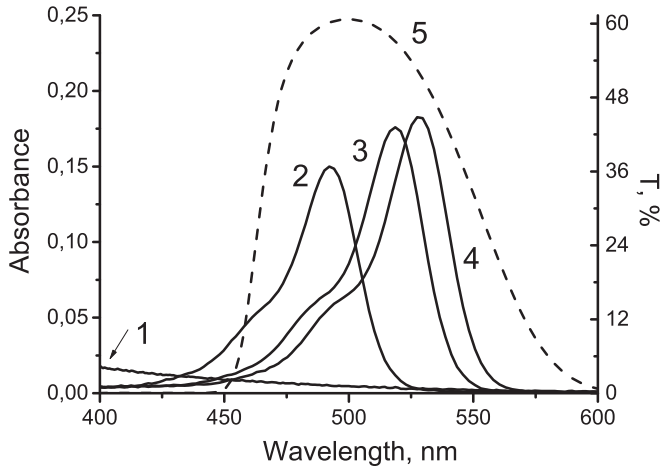

Fig. 2. Absorption spectra of PFD (1), fluorescein (2), eosin Y (3) and erythrosin B (4) at a concentration of $2 \cdot 10^{-6}$ M in water (pH = 6.5). Filter transparency is also shown (5).

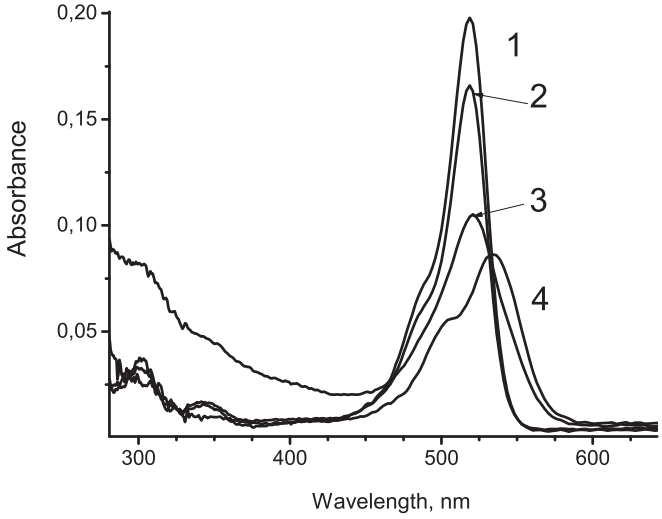

Fig. 3. Absorption spectra of eosin Y ($2 \cdot 10^{-6}$ M in water): in the absence of a quencher (1) and in the presence of PFD in concentrations of $0.7 \cdot 10^{-6}$ (2), $2 \cdot 10^{-6}$ (3), calculated eosin Y spectrum in XD-PFD complex (4).

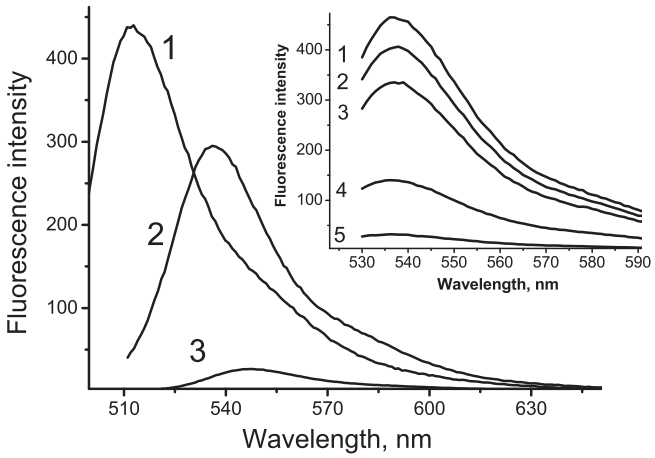

Fig. 4. Fluorescence spectra of fluorescein (1), erythrosin B (2) and eosin Y (3) at a concentration of $2\cdot10^{-6}$ M in water (pH = 6.5). λ_{ex} = 490 nm (fluorescein), 518 nm (eosin), 530 nm (erythrosin). **In the inset**: Fluorescence spectra of eosin Y ($2\cdot10^{-6}$ M in water): (1) in the absence of a quencher and in the presence of PFD in concentrations of $4.8\cdot10^{-7}$ M, $9.1\cdot10^{-7}$ M, $2\cdot10^{-6}$ M and $2.86\cdot10^{-6}$ M (2–5).

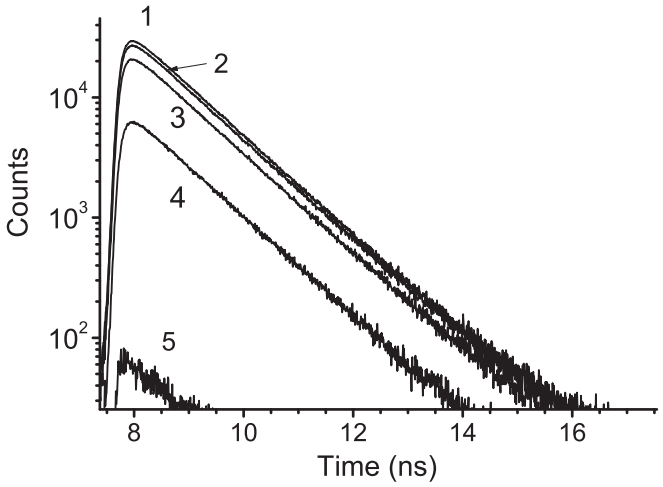

Fig. 5. Fluorescence decay profiles for $5\cdot10^{-6}$ M water solution of eosin Y: in the absence of a quencher (1); in the presence of the PFD in concentrations $2.4\cdot10^{-7}$, $9\cdot10^{-7}$, $2.6\cdot10^{-6}$ and $5\cdot10^{-6}$ (2–5) in water (pH = 6.5), λ_{ex} = 518 nm, λ_{em} = 540 nm.

determining the equilibrium constant of the XD-PFD complex (Table 1) from the linear part of dependence (at the minimal PFD concentrations). The deviation of Stern-Volmer graphs from the linear with PFD concentration increasing can be explained by the formation of large XD-PFD associates.

The evidence of the formation of fullerene associates in aqueous solution was shown by dynamic light scattering for similar fullerene derivatives [57]. Another evidence of the formation of fullerene associates is shown on Fig. 7. Effective quenching of eosin Y fluorescence is observed when increasing of PFD concentrations administered sequentially to eosin Y solution. This process is displayed in the Stern-Volmer coordinates by a nonlinear dependence 1. Then, the solution with maximal PFD concentration was diluted successively with water, whereby the concentration of eosin Y and PFD in the cuvette decreased. This reduces the intensity of the fluorescence of the sample.

Taking into account the dilution of the fluorophore, the analysis of this process in the Stern-Volmer coordinates gives a curve 2, which is significantly different from curve 1 (Fig. 7). If we fix the concentration of the components in the process of dilution, the degree of quenching (and thus the association) returned slowly to the value, which was observed at the elevation of the PFD concentration (arrow 3). The inset shows the points corresponding to maintaining the solution at a given concentration for 15, 22 and 46 h. The observed hysteresis can be explained by the rapid formation of associates with increasing concentration of PFD and their slow dissociation at lower concentrations.

The nature of the interaction of XD with PFD in the presence of liposomes varies considerably. As can be seen from Fig. 6B the shape of Stern-Volmer dependence for dyes in liposomes becomes considerably more linear, indicating the dissociation of the nanostructures in liposomes.

From the data on the quenching of steady-state fluorescence, suggesting that the fluorescence of the XD in the complex is carried out to zero, it is possible to determine the fraction of free XD molecules in solution at various concentrations of the PFD. Using these data of the absorption spectra of samples the absorption spectrum of the XD in XD-PFD complex can be calculated as shown for eosin Y-PFD complex (Fig. 3, curve 4). As can be seen from this curve, the maximum absorption spectrum of eosin Y in the complex with fullerene is shifted from 517 nm to 527 nm, and the extinction coefficient decreases from $8.03\cdot10^4$ $M^{-1}cm^{-1}$ to $4.06\cdot10^4$ $M^{-1}cm^{-1}$.

Taking into account the spectral and donor-acceptor properties of fullerenes, one can assume two mechanisms of XD fluorescence quenching in the XD-PFD complex – by the inductive-resonance dipole-dipole energy transfer and by electron transfer mechanisms. It is known that the inductive-resonant dipole-dipole energy transfer is carried out in the presence of the overlap of the luminescence spectra of the donor (XD) and acceptor (PFD). As seen from Figs. 3 and 4, such an overlap occurs, though the PFD has rather small absorption in the range of 500–650 nm.

According to the Förster theory [72], in the case of inductive-resonance dipole-dipole energy transfer the formula

$$R_0^6 = 8.79\times10^{-5}\left(\kappa^2 n^{-4} Q_D J(\lambda)\right), (R_0 \text{ in A, if } \lambda[\text{nm}]) \quad (1)$$

can be used for the calculation of the R_0 value: the distance at which the fluorescence quenching should take place by 50%. In formula (1), Q_d is the quantum yield of the donor fluorescence in the absence of acceptor, $J(\lambda)$ is the overlap integral, n is the refractive index of the solvent, and k is the orientation coefficient depending on the directions of the dipole moments of the transition. In systems with the disordered orientations of the dipole moments of the transition, it is usually assumed that $k^2 = 2/3$.

With knowledge of the R_0 value and the efficiency of fluorescence quenching due to the excitation transfer from the donor to the acceptor, which is expressed by the ratio I_0/I, where I_0 is the fluorescence intensity in the absence of the acceptor and I is the fluorescence intensity in the presence of the acceptor, the formula

$$R = \frac{R_0}{\sqrt[6]{\frac{I_0}{I}-1}} \quad (2)$$

can be used to determine the distance R between the donor and acceptor.

As was shown from the experimental results, using the formula (1) with the value Q_d of fluorescence quantum yields, listed in Table 1, and n = 1.33, the R_0 values for the investigated pairs XD-PFD are in the range 20–38 Å (Table 1). It was shown from the experiment that during the formation of the XD-PFD the fluorescence intensity of the dyes is decreased almost by 1000 times (Fig. 4). Using formula (2), it is possible to determine that the

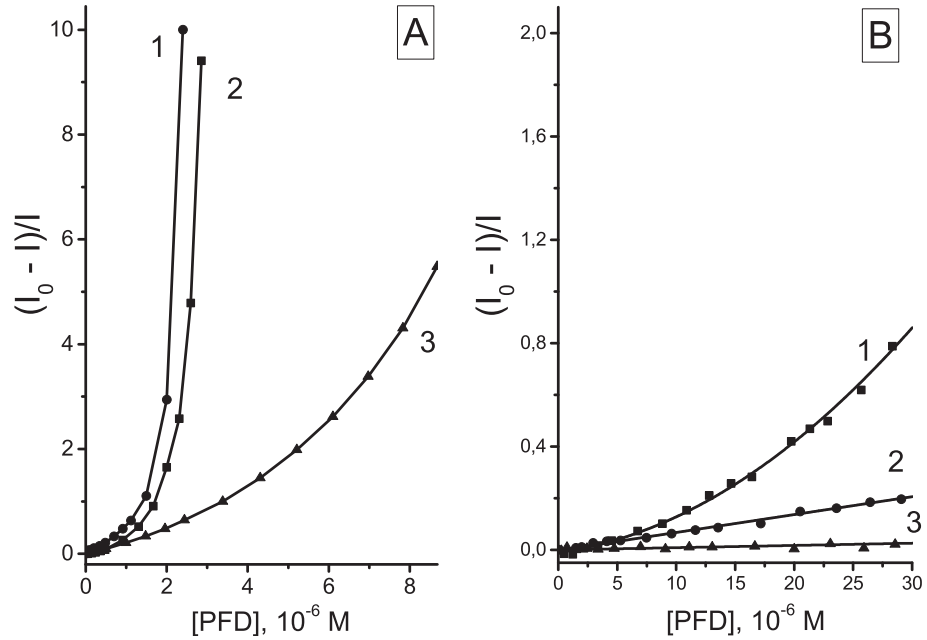

Fig. 6. The influence of PFD on the fluorescence spectra intensity of erythrosin B (1), eosin Y (2) and fluorescein (3) in Stern-Volmer coordinates in water (**A**) and in the structure of liposomes (**B**). Dye concentration $2 \cdot 10^{-6}$ M.

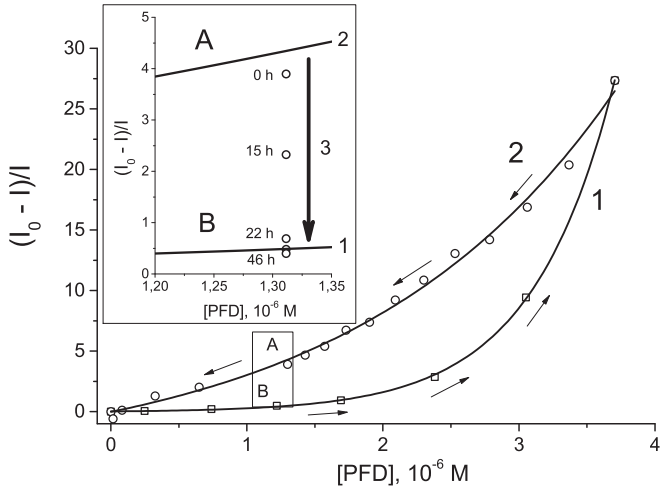

Fig. 7. Quenching of the eosin Y fluorescence intensity with PFD: gradual addition of PFD to eosin Y (1); gradual dilution of mixture «eosin Y + PFD» with water (2). **In the inset**: change in fluorescence intensity of the solution of «eosin Y + PFD» mixture taken at points A with a different exposure time (time specified in hours, arrow 3). The graphs are constructed in the Stern-Volmer coordinates. All compounds were dissolved in water, pH 6.5.

distance between XD molecule and the fullerene core in the formed complex is shorter than 7–13 Å. This agrees well with the spatial structure of HNS in which the dye interacts with the fullerene derivative in the places of the charge contacts. They are separated by hydrocarbon chains containing four chemical bonds (~5–6 Å). On the basis of this, it is possible to assume that the inductive resonance quenching mechanism can be one of the main channels of the deactivation of XD with the energy transfer to the fullerene core.

The second mechanism of deactivation of the singlet state of the dye could be the quenching by electron transfer. According to the Marcus theory the electron transfer constant between donor and acceptor k_{et} is determined by formula

$$k_{et} = k_0 \, exp\left(-\frac{(\Delta G + \lambda)^2}{4\lambda k_B T} \right) \tag{3}$$

where

$$k_0 = \frac{2\pi V_{ab}^2(R)}{\hbar\sqrt{4\pi\lambda k_B T}} \tag{4}$$

$$V_{ab}(R) = V_0 \exp\left(-\frac{R}{\hbar}\sqrt{2mH} \right) \tag{5}$$

In these expressions: k_0– preexponential factor, V_{ab} – overlapping integral characterizing quantum effect of wave functions overlapping of the donor and acceptor, ΔG – the free energy of the reaction, λ – nuclear energy reorganization, $\hbar$ – Planck's constant, k_B – Boltzmann constant, H and R – barrier height and the distance of tunneling [73,74].

According to formulas (3)–(5), k_{et} depends exponentially on the distance R, the free energy ΔG and nuclear energy reorganization λ. Under optimal reaction conditions, to estimate the rate of electron transfer reaction the formula (6) can be applied

$$k_{et} = k_0 exp(-\alpha R) \tag{6}$$

which was obtained as a result of generalization of the electron transfer data in a various molecular structures, including photo-excited molecules [75–77]. Here $k_0 = 10^{13}$ s^{-1}, R – the distance between the donor and acceptor, α – parameter characterizing the influence of the environment on the overlap of the donor and acceptor wave functions overlapping due superexchange interaction. Depending on the type of matrix, separating the donor and acceptor (saturated hydrocarbon chain, the polypeptide chain, packed in different ways, water or vacuum), the value α may be 0.9 $Å^{-1}$ for saturated hydrocarbon chains, 1.4 $Å^{-1}$ for protein globules, 1.8–2.4 $Å^{-1}$ – for the water molecules [78].

It was found that lifetimes of the excited singlet state of the dye

in the experiment are in the range 0.09–3.6 ns (Table 1). Considering the fact that fluorescence intensity is about 1000 times quenched, it can be estimated from equation (6) that the electron transfer from the excited dye to the fullerene can take place at a distance of 5.1 Å at optimal values of ΔG and λ in 10 ps along the saturated hydrocarbon chain ($\alpha = 0.9$ Å^{-1}). The given result also corresponds to the proposed structure of the complex.

Thus, the analysis of the dye fluorescence quenching in the complex indicates that the quenching of the excited singlet state can occur due to the transfer of excitation or by the mechanism of electron transfer, which does not allow making an unambiguous conclusion about the superiority of one of the quenching mechanism. However, in any case, dye fluorescence quenching in the complex with fullerene derivative means that there is an effective transfer of excitation or electron to the fullerene core, which should give fullerene the ability to generate reactive oxygen species.

3.2. Study of photochemical activity of PFD complexes with XD in aqueous solutions and in the structure of the liposomes

To clarify the pathway of reactive oxygen species (ROS) generation in aqueous solutions by water-soluble dye-fullerene complexes the comparative efficacy of superoxide radical generation $O_2^{\bullet -}$ by XD-PFD complexes was investigated using fluorescein, eosin Y and erythrosin B.

Fig. 8 shows an example of photodynamic activity studies of eosin Y, PFD and their mixed solution. As can be seen from Fig. 8, eosin Y and PFD have detectable photodynamic activity upon photoexcitation in the 450–550 nm region (Fig. 2, curve 5). Taking into account the difference in the extinction coefficient in the range of excitation wavelengths, it can be estimated that the photodynamic activity of PFD in relation to one absorbed quantum exceeds the similar activity of eosin about 30 times.

Addition of eosin Y to PFD solution in equimolar concentration resulted in a significant increase of the rate of the photochemical reaction compared with photodynamic activity of individual compounds. In this case, the reaction rate is 3.2 times greater than the sum of the individual contributions of these compounds in the overall response rate (Fig. 8). Obviously, this is due to the interaction of these compounds in solution. Determining from the fluorescence quenching data that only 63% of the dye molecules are in the complex PFD-eosin Y, and taking into account that extinction coefficient of the dye in the complex is reduced, it can be estimated that the relative quantum yield of photochemical reaction $O_2^{\bullet -}$ generation for such complexes is 7.3 times greater than for the individual dye and 10 times larger than that for the PFD.

Another remarkable effect of the formation of XD-PFD complexes is the increased photostability of dyes. As an example, Fig. 9 shows the dependence of absorption intensity of eosin Y on the irradiation time in the presence and absence of PFD. Fig. 9 shows that in a reaction mixture with NADH and EDTA, the absorption maximum of eosin Y is sharply reduced upon irradiation in the absorption band of the dye, while in the presence of PFD absorption reduction is much more slowly.

Table 1 shows a comparison of the relative photochemical activity of complexes of PFD with fluorescein, eosin Y and erythrosin B under identical experimental conditions.

The following formula

$$E_c = \frac{D_{complex} - D_{control}}{(D_{PFD} - D_{control}) + \left(D_{dye} - D_{control}\right)} \quad (7)$$

was used to calculate enhancing coefficient E_c of the relative photochemical activity of the XD-PFD complex in water and in liposomes, were index D is a $_{\Delta}D_{560}$ for studied compounds after 5 min of photoirradiation. Table 1 shows that the photochemical activity of these complexes is decreased in a line of fluorescein > eosin Y > erythrosin B. Taking into account that quantum yields for singlet state fluorescein, eosin Y and erythrosin B are 0.93, 0.68 and 0.03, respectively, one can conclude that the main role in the photochemical processes are playing exactly the singlet excited states of the dyes. Similar effect was described for non-covalent fullerene-dye complexes and covalent dyads in non-polar solvents [29,39–41,47,48,79], but for aqueous solutions it hasn't been reported before, to our best knowledge.

It may be supposed, that low E_c values for XD-PFD complexes in liposomes (Table 1) are related to dissociation of XD-PFD complexes due to pronounced membranotropic properties of water-soluble fullerene derivatives [80]. Given results are in a good agreement with Stern-Volmer dependences for XD-PFD complexes in water and liposomes (Fig. 6A and B).

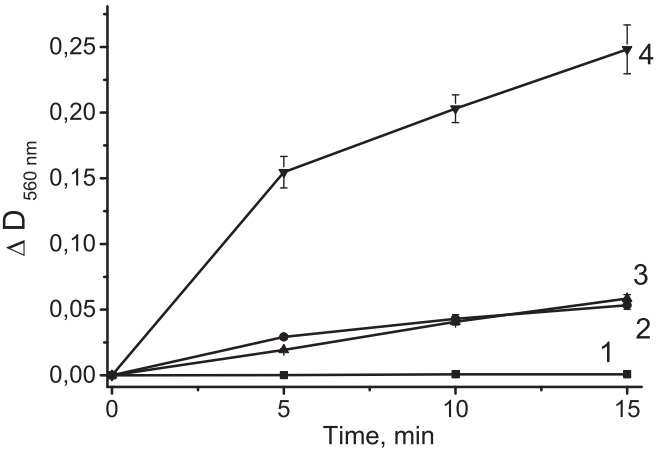

Fig. 8. Kinetics of $O_2^{\bullet -}$ formation as a result of the photochemical reaction under visible light irradiation in the range of 450–550 nm. The data points were obtained by monitoring the changes in the optical density ΔD of the solution at 560 nm (the formazan absorption band maximum) and plotted as a function of the irradiation time: control (1), sensitization with eosin Y (2), sensitization with PFD (3), sensitization with eosin Y + PFD (4). All compounds are at a concentration of $2 \cdot 10^{-6}$ M in water (pH 6.5).

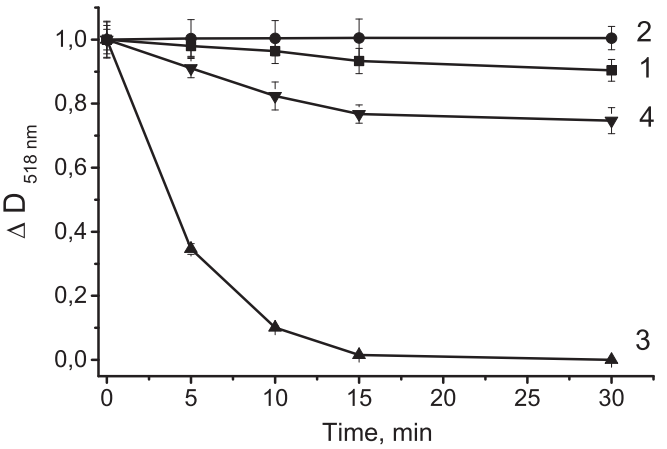

Fig. 9. Changes in absorption of eosin Y in the presence of various compounds: eosin Y ($2 \cdot 10^{-6}$ M) (1); eosin Y ($2 \cdot 10^{-6}$ M) + PFD ($2 \cdot 10^{-6}$ M) (2); eosin Y ($2 \cdot 10^{-6}$ M) + EDTA ($2 \cdot 10^{-5}$ M) + NADH ($4 \cdot 10^{-4}$ M) (3); eosin Y ($2 \cdot 10^{-6}$ M) + PFD ($2 \cdot 10^{-6}$ M) + EDTA ($2 \cdot 10^{-5}$ M) + NADH ($4 \cdot 10^{-4}$ M) (4). All compounds were dissolved in Tris-HCl buffer (0.01 M; pH 7.4).

4. Conclusion

Thus, based on the obtained experimental data, it can be concluded that polycationic fullerene derivative and xanthene dyes formed strong complexes in aqueous solution. Observed photodynamic activity such complexes significantly exceed one of individual molecules PFD and dyes upon photoexcitation complexes at the dye absorption band.

Analysis of the fluorescence quenching effect of fluorescein, eosin Y and erythrosin B in the complex with the PFD shows that the quenching of the excited singlet state of these xanthene dyes can occur due to the transfer of excitation or by the electron transfer mechanism, which gives to fullerene the ability to generate reactive oxygen species.

It is usually assumed that eosin Y and other dyes generate reactive oxygen species due to the energy or electron transfer from the triplet levels of dyes. In the present work it has been shown that the fullerene core in the complex structure allows transforming the singlet excitation of the dye in generation of reactive oxygen species with high efficiency.

The creation of such hybrid nanostructures based on fullerenes and dyes that absorb in the visible region of the spectrum may be promising in terms of creating new and effective photosensitizers for use in medicine and photocatalysis.

Acknowledgements

This work was supported by the Research Program of the Presidium of Russian Academy of Sciences No 1 ≪Nanostructures: physics, chemistry, biology and basic technology≫ (grants awarded to Prof. A.I. Kotelnikov and Dr. P.A. Troshin), Russian Foundation for Basic Research (grants Nos. 15-29-01200-OFI-m and 16-34-01156 mol_a), and by FP7-PEOPLE-2013-IRSES project “Multicoloured ambipolar conducting polymers for single polymer optoelectronic devices” (AmbiPOD, Grant agreement no.: PIRSES-GA-2013-612670).

References

[1] Allison RR. Photodynamic therapy: oncologic horizons. Futur Oncol 2014;10:123–4. http://dx.doi.org/10.2217/fon.13.176.
[2] Agostinis P, Berg K, Cengel KA, Foster TH, Girotti AW, Gollnick SO, et al. Photodynamic therapy of cancer: an update. CA Cancer J Clin 2011;61:250–81. http://dx.doi.org/10.3322/caac.20114.
[3] Sharma SK, Mroz P, Dai T, Huang Y-Y, St Denis TG, Hamblin MR. Photodynamic therapy for Cancer and for infections: what is the difference? Isr J Chem 2012;52:691–705. http://dx.doi.org/10.1002/ijch.201100062.
[4] Castrucci JS, Josey DS, Thibau E, Lu Z-H, Bender TP. Boron subphthalocyanines as triplet harvesting materials within organic photovoltaics. J Phys Chem Lett 2015;6:3121–5. http://dx.doi.org/10.1021/acs.jpclett.5b01254.
[5] Gudeika D, Grazulevicius JV, Volyniuk D, Juska G, Jankauskas V, Sini G. Effect of ethynyl linkages on the properties of the derivatives of triphenylamine and 1,8-Naphthalimide. J Phys Chem C 2015;119:28335–46. http://dx.doi.org/10.1021/acs.jpcc.5b10163.
[6] Xu Z, Li Y, Ma X, Gao X, Tian H. Synthesis and properties of iridium complexes based 1,3,4-oxadiazoles derivatives. Tetrahedron 2008;64:1860–7. http://dx.doi.org/10.1016/j.tet.2007.11.099.
[7] Encinas MV, Rufs AM, Bertolotti SG, Previtali CM. Xanthene dyes/amine as photoinitiators of radical polymerization: a comparative and photochemical study in aqueous medium. Polym Guildf 2009;50:2762–7. http://dx.doi.org/10.1016/j.polymer.2009.04.024.
[8] Cui X, Zhang C, Xu K, Zhao J. Application of singlet energy transfer in triplet state formation: broadband visible light-absorbing triplet photosensitizers, molecular structure design, related photophysics and applications. J Mater Chem C 2015;3:8735–59. http://dx.doi.org/10.1039/C5TC01401H.
[9] Ma D-L, Ma VP-Y, Chan DS-H, Leung K-H, He H-Z, Leung C-H. Recent advances in luminescent heavy metal complexes for sensing. Coord Chem Rev 2012;256:3087–113. http://dx.doi.org/10.1016/j.ccr.2012.07.005.
[10] Barinov AV, Goryachev NS, Kotel'nikov AI. Analysis of microsecond relaxation dynamics of proteins and viscous media by recording relaxation shifts of phosphorescence spectra. Opt Spectrosc 2011;110:724–9. http://dx.doi.org/10.1134/S0030400X11050043.
[11] Likhtenstein GI, Kulikov AV, Kotelnikov AI, Levchenko LA. Methods of physical labels - a combined approach to the study of microstructure and dynamics in biological systems. J Biochem Biophys Methods 1986;12:1–28. http://dx.doi.org/10.1016/0165-022X(86)90047-3.
[12] Wu W, Guo H, Wu W, Ji S, Zhao J. Organic triplet sensitizer library derived from a single chromophore (BODIPY) with long-lived triplet excited state for triplet-triplet annihilation based upconversion. J Org Chem 2011;76:7056–64. http://dx.doi.org/10.1021/jo200990y.
[13] Plaetzer K, Krammer B, Berlanda J, Berr F, Kiesslich T. Photophysics and photochemistry of photodynamic therapy: fundamental aspects. Lasers Med Sci 2009;24:259–68. http://dx.doi.org/10.1007/s10103-008-0539-1.
[14] Koeppe R, Sariciftci NS. Photoinduced charge and energy transfer involving fullerene derivatives. Photochem Photobiol Sci 2006;5:1122–31. http://dx.doi.org/10.1039/b612933c.
[15] Mroz P, Pawlak A, Satti M, Lee H, Wharton T, Gali H, et al. Functionalized fullerenes mediate photodynamic killing of cancer cells: type I versus Type II photochemical mechanism. Free Radic Biol Med 2007;43:711–9. http://dx.doi.org/10.1016/j.freeradbiomed.2007.05.005.
[16] Yamakoshi Y, Umezawa N, Ryu A, Arakane K, Miyata N, Goda Y, et al. Active oxygen species generated from photoexcited fullerene (C60) as potential medicines: $O_2^{\bullet}$ versus $^1O_2$. J Am Chem Soc 2003;125:12803–9. http://dx.doi.org/10.1021/ja0355574.
[17] Patel MB, Harikrishnan U, Valand NN, Mehta DS, Joshi KV, Kumar SP, et al. Novel cationic fullerene derivatized s-triazine scaffolds as photoinduced DNA cleavage agents: design, synthesis, biological evaluation and computational investigation. RSC Adv 2013;3:8734. http://dx.doi.org/10.1039/c3ra40950c.
[18] Sharma SK, Chiang LY, Hamblin MR. Photodynamic therapy with fullerenes in vivo: reality or a dream? Nanomed Lond 2011;6:1813–25. http://dx.doi.org/10.2217/nnm.11.144.
[19] Fan J, Fang G, Zeng F, Wang X, Wu S. Water-dispersible fullerene aggregates as a targeted anticancer prodrug with both chemo- and photodynamic therapeutic actions. Small 2013;9:613–21. http://dx.doi.org/10.1002/smll.201201456.
[20] Mroz P, Tegos GP, Gali H, Wharton T, Sarna T, Hamblin MR. Photodynamic therapy with fullerenes. Photochem Photobiol Sci 2007;6:1139–49. http://dx.doi.org/10.1039/b711141j.
[21] Doi Y, Ikeda A, Akiyama M, Nagano M, Shigematsu T, Ogawa T, et al. Intracellular uptake and photodynamic activity of water-soluble [60]- and [70] fullerenes incorporated in liposomes. Chemistry 2008;14:8892–7. http://dx.doi.org/10.1002/chem.200801090.
[22] Hu Z, Zhang C, Huang Y, Sun S, Guan W, Yao Y. Photodynamic anticancer activities of water-soluble C(60) derivatives and their biological consequences in a HeLa cell line. Chem Biol Interact 2012;195:86–94. http://dx.doi.org/10.1016/j.cbi.2011.11.003.
[23] Huang L, Wang M, Sharma SK, Sperandio FF, Maragani S, Nayka S, et al. Decacationic [70]Fullerene approach for efficient photokilling of infectious bacteria and Cancer cells. ECS Trans 2013;45:1–11. http://dx.doi.org/10.1149/04520.0065ecst.
[24] Milanesio ME, Spesia MB, Cormick MP, Durantini EN. Mechanistic studies on the photodynamic effect induced by a dicationic fullerene C_{60} derivative on Escherichia coli and Candida albicans cells. Photodiagn Photodyn Ther 2013;10:320–7. http://dx.doi.org/10.1016/j.pdpdt.2013.01.007.
[25] Mizuno K, Zhiyentayev T, Huang L, Khalil S, Nasim F, Tegos GP, et al. Antimicrobial photodynamic therapy with functionalized fullerenes: quantitative structure-activity relationships. J Nanomed Nanotechnol 2011;2:1–9. http://dx.doi.org/10.4172/2157-7439.1000109.
[26] Wang M, Maragani S, Huang L, Jeon S, Canteenwala T, Hamblin MR, et al. Synthesis of decacationic [60]fullerene decaiodides giving photoinduced production of superoxide radicals and effective PDT-mediation on antimicrobial photoinactivation. Eur J Med Chem 2013;63:170–84. http://dx.doi.org/10.1016/j.ejmech.2013.01.052.
[27] Lu Z, Dai T, Huang L, Kurup DB, Tegos GP, Jahnke A, et al. Photodynamic therapy with a cationic functionalized fullerene rescues mice from fatal wound infections. Nanomed Lond 2010;5:1525–33. http://dx.doi.org/10.2217/nnm.10.98.
[28] D'Souza F, Smith PM, Zandler ME, McCarty AL, Itou M, Araki Y, et al. Energy transfer followed by electron transfer in a supramolecular triad composed of boron dipyrrin, zinc porphyrin, and fullerene: a model for the photosynthetic antenna-reaction center complex. J Am Chem Soc 2004;126:7898–907. http://dx.doi.org/10.1021/ja030647u.
[29] Berera R, Moore GF, van Stokkum IHM, Kodis G, Liddell P a, Gervaldo M, et al. Charge separation and energy transfer in a caroteno-C_{60} dyad: photoinduced electron transfer from the carotenoid excited states. Photochem Photobiol Sci 2006;5:1142–9. http://dx.doi.org/10.1039/b613971j.
[30] Guo S, Xu L, Xu K, Zhao J, Küçüköz B, Karatay A, et al. Bodipy–C_{60} triple hydrogen bonding assemblies as heavy atom-free triplet photosensitizers: preparation and study of the singlet/triplet energy transfer. Chem Sci 2015;6:3724–37. http://dx.doi.org/10.1039/C4SC03865G.
[31] Hua J, Meng F, Ding F, Li F, Tian H. Novel soluble and thermally-stable fullerene dyad containing perylene. J Mater Chem 2004;14:1849. http://dx.doi.org/10.1039/b316996k.
[32] Zhao J, Xu K, Yang W, Wang Z, Zhong F. The triplet excited state of Bodipy: formation, modulation and application. Chem Soc Rev 2015;44:8904–39. http://dx.doi.org/10.1039/C5CS00364D.
[33] Huang L, Zhao J. Switching of the triplet excited state of the C_{60}-dimethylaminostyryl BODIPY dyads/triads. J Mater Chem C Mater Opt Electron Devices

2015;3:538–50. http://dx.doi.org/10.1039/C4TC02037E.
[34] Ziessel R, Allen BD, Rewinska DB, Harriman A. Selective triplet-state formation during charge recombination in a fullerene/bodipy molecular dyad (Bodipy=Borondipyrromethene). Chem A Eur J 2009;15:7382–93. http://dx.doi.org/10.1002/chem.200900440.
[35] Li C-Z, Yip H-L, Jen AK-Y. Functional fullerenes for organic photovoltaics. J Mater Chem 2012;22:4161. http://dx.doi.org/10.1039/c2jm15126j.
[36] Krokos E, Spänig F, Ruppert M, Hirsch A, Guldi DM. A charge-transfer challenge: combining fullerenes and metalloporphyrins in aqueous environments. Chemistry 2012;18:1328–41. http://dx.doi.org/10.1002/chem.201102851.
[37] Nadtochenko NA, Denisov NN, Levin PP. Dynamics of contact radical ion pairs C60—aromatic amines. A study by picosecond laser photolysis. Russ Chem Bull 1995;44:1038–49. http://dx.doi.org/10.1007/BF00707050.
[38] Megiatto JD, Schuster DI, de Miguel G, Wolfrum S, Guldi DM. Topological and conformational effects on electron transfer dynamics in Porphyrin-[60]Fullerene interlocked systems. Chem Mater 2012;24:2472–85. http://dx.doi.org/10.1021/cm3004408.
[39] Ray A, Pal H, Bhattacharya S. Photophysical investigations on supramolecular fullerene/phthalocyanine charge transfer interactions in solution. Spectrochim Acta A Mol Biomol Spectrosc 2014;117:686–95. http://dx.doi.org/10.1016/j.saa.2013.08.107.
[40] Halder A, Bhatt S, Nayak SK, Chattopadhyay S, Bhattacharya S. UV-Vis, fluorescence and NMR spectroscopic investigations on inclusion properties of a designed tetrahomocalix[8]arene with fullerenes C_{60} and C_{70} in solution. Spectrochim Acta A Mol Biomol Spectrosc 2011;84:25–31. http://dx.doi.org/10.1016/j.saa.2011.08.011.
[41] Wilson SR, MacMahon S, Tat FT, Jarowski PD, Schuster DI. Synthesis and photophysics of a linear non-covalently linked porphyrin–fullerene dyad. Chem Commun 2003;2:226–7. http://dx.doi.org/10.1039/b208013c.
[42] Tkachenko NV, Efimov A, Lemmetyinen H. Covalent phthalocyanine-fullerene dyads: synthesis, electron transfer in solutions and molecular films. J Porphyr Phthalocyanines 2011;15:780–90. http://dx.doi.org/10.1142/S1088424611003732.
[43] Maligaspe E, Tkachenko NV, Subbaiyan NK, Chitta R, Zandler ME, Lemmetyinen H, et al. Photosynthetic antenna-reaction center mimicry: sequential energy- and electron transfer in a self-assembled supramolecular triad composed of boron dipyrrin, zinc porphyrin and fullerene. J Phys Chem A 2009;113:8478–89. http://dx.doi.org/10.1021/jp9032194.
[44] Garg V, Kodis G, Chachisvilis M, Hambourger M, Moore AL, Moore TA, et al. Conformationally constrained macrocyclic diporphyrin-fullerene artificial photosynthetic reaction center. J Am Chem Soc 2011;133:2944–54. http://dx.doi.org/10.1021/ja1083078.
[45] Shi W-J, El-Khouly ME, Ohkubo K, Fukuzumi S, Ng DKP. Photosynthetic antenna-reaction center mimicry with a covalently linked monostyryl boron-dipyrromethene-aza-boron-dipyrromethene-C_{60} triad. Chemistry 2013;19:11332–41. http://dx.doi.org/10.1002/chem.201300318.
[46] D'Souza F, Wijesinghe CA, El-Khouly ME, Hudson J, Niemi M, Lemmetyinen H, et al. Ultrafast excitation transfer and charge stabilization in a newly assembled photosynthetic antenna-reaction center mimic composed of boron dipyrrin, zinc porphyrin and fullerene. Phys Chem Chem Phys 2011;13:18168–78. http://dx.doi.org/10.1039/c1cp90147h.
[47] Liu Y, Zhao J. Visible light-harvesting perylenebisimide-fullerene (C_{60}) dyads with bidirectional “ping-pong” energy transfer as triplet photosensitizers for photooxidation of 1,5-dihydroxynaphthalene. Chem Commun Camb 2012;48:3751–3. http://dx.doi.org/10.1039/c2cc30345k.
[48] Remón P, Carvalho P, Baleizo C, Berberan MN, Parente Carvalho C, Baleizão C, et al. Highly efficient singlet-singlet energy transfer in light-harvesting [60,70]fullerene-4-amino-1,8-naphthalimide dyads. Chemphyschem 2013;3:2717–24. http://dx.doi.org/10.1002/cphc.201300424.
[49] Yamakoshi YN, Yagami T, Sueyoshi S, Miyata N. Acridine adduct of [60]Fullerene with enhanced DNA-cleaving activity. J Org Chem 1996;61:7236–7. http://dx.doi.org/10.1021/jo961210q.
[50] Milanesio ME, Alvarez MG, Rivarola V, Silber JJ, Durantini EN. Porphyrin-fullerene C_{60} dyads with high ability to form photoinduced charge-separated state as novel sensitizers for photodynamic therapy. Photochem Photobiol 2005;81:891–7. http://dx.doi.org/10.1562/2005-01-24-RA-426.
[51] Alvarez MG, Prucca C, Milanesio ME, Durantini EN, Rivarola V. Photodynamic activity of a new sensitizer derived from porphyrin-C_{60} dyad and its biological consequences in a human carcinoma cell line. Int J Biochem Cell Biol 2006;38:2092–101. http://dx.doi.org/10.1016/j.biocel.2006.05.019.
[52] Ballatore MB, Spesia MB, Milanesio ME, Durantini EN. Synthesis, spectroscopic properties and photodynamic activity of porphyrin-fullerene C_{60} dyads with application in the photodynamic inactivation of Staphylococcus aureus. Eur J Med Chem 2014;83:685–94. http://dx.doi.org/10.1016/j.ejmech.2014.06.077.
[53] Constantin C, Neagu M, Ion R-M, Gherghiceanu M, Stavaru C. Fullerene-porphyrin nanostructures in photodynamic therapy. Nanomed Lond 2010;5:307–17. http://dx.doi.org/10.2217/nnm.09.111.
[54] Okuda K, Abeta C, Hirota T, Mochizuki M, Mashino T. Synthesis of water-soluble C_{60}-porphyrin hybrid compounds. Chem Pharm Bull Tokyo 2002;50:985–7. http://dx.doi.org/10.1248/cpb.50.985.
[55] Lu F, Haque SA, Yang S-T, Luo PG, Gu L, Kitaygorodskiy A, et al. Aqueous compatible fullerene-doxorubicin conjugates. J Phys Chem C Nanomater Interfaces 2009;113:17768. http://dx.doi.org/10.1021/jp906750z.
[56] Zhou C, Liu Q, Xu W, Wang C, Fang X. A water-soluble C_{60}-porphyrin compound for highly efficient DNA photocleavage. Chem Commun Camb 2011;47:2982–4. http://dx.doi.org/10.1039/c0cc04919k.
[57] Kotelnikov AI, Rybkin AY, Khakina EA, Kornev AB, Barinov AV, Goryachev NS, et al. Hybrid photoactive fullerene derivative-ruboxyl nanostructures for photodynamic therapy. Org Biomol Chem 2013;11:4397–404. http://dx.doi.org/10.1039/c3ob40136g.
[58] Sperandio FF, Sharma SK, Wang M, Jeon S, Huang Y-Y, Dai T, et al. Photoinduced electron-transfer mechanisms for radical-enhanced photodynamic therapy mediated by water-soluble decacationic C_{70} and $C_{84}O_2$ Fullerene Derivatives. Nanomedicine 2013;9:570–9. http://dx.doi.org/10.1016/j.nano.2012.09.005.
[59] Yin R, Wang M, Huang Y-Y, Huang H-C, Avci P, Chiang LY, et al. Photodynamic therapy with decacationic [60]fullerene monoadducts: effect of a light absorbing electron-donor antenna and micellar formulation. Nanomedicine 2014;10:795–808. http://dx.doi.org/10.1016/j.nano.2013.11.014.
[60] Troshin PA, Troshina OA, Peregudova SM, Yudanova EI, Buyanovskaya AG, Konarev DV, et al. Chemical and electrochemical reduction of the highly chlorinated fullerenes $C_{60}Cl_{24}$ and $C_{60}Cl_{30}$. Mendeleev Commun 2006;16:206–8. http://dx.doi.org/10.1070/MC2006v016n04ABEH002346.
[61] Amat-Guerri F, López-González MMC, Sastre R, late R. Martinez-Utrilla T. Spectrophotometric determination of ionization and isomerization constants of Rose Bengal, eosin Y and some derivatives. Dye Pigment 1990;13:219–32. http://dx.doi.org/10.1016/0143-7208(90)80021-G.
[62] Klonis N, Sawyer WH. Spectral properties of the prototropic forms of fluorescein in aqueous solution. J Fluoresc 1996;6:147–57. http://dx.doi.org/10.1007/BF00732054.
[63] Parker CA. Phosphorescence and delayed fluorescence from solutions. Advances photochem, vol. 2. New York,: Wiley (Interscience); 1964. p. 305–83. http://dx.doi.org/10.1002/9780470133323.ch8.
[64] Hebbink GA, Grave L, Woldering LA, Reinhoudt DN, Van Veggel FCJM. Unexpected sensitization efficiency of the near-infrared Nd^{3+}, Er^{3+}, and Yb^{3+} emission by fluorescein compared to eosin and erythrosin. J Phys Chem A 2003;107:2483–91. http://dx.doi.org/10.1021/jp0260090.
[65] Arbogast JW, Darmanyan AP, Foote CS, Diederich FN, Whetten RL, Rubin Y, et al. Photophysical properties of sixty atom carbon molecule (C_{60}). J Phys Chem 1991;95:11–2. http://dx.doi.org/10.1021/j100154a006.
[66] Chrysochoos J, Shihabi DS. X-radiolysis of aqueous erythrosin. Radiat Res 1971;47:392–401.
[67] Redmond RW, Gamlin JN. A compilation of singlet oxygen yields from biologically relevant molecules. Photochem Photobiol 1999;70:391–475. http://dx.doi.org/10.1111/j.1751-1097.1999.tb08240.x.
[68] Rooijen NV, Sanders A. Liposome mediated depletion of macrophages: mechanism of action, preparation of liposomes and applications. J Immunol Methods 1994;174:83–93. http://dx.doi.org/10.1016/0022-1759(94)90012-4.
[69] Porter G, Reid ES, Tredwell CJ. Time resolved fluorescence in the picosecond region. Chem Phys Lett 1974;29:469–72. http://dx.doi.org/10.1016/0009-2614(74)85147-X.
[70] Boens NN, Qin W, Basarić N, Hofkens J, Ameloot M, Pouget J, et al. Fluorescence lifetime standards for time and frequency domain fluorescence spectroscopy. Anal Chem 2007;79:2137–49. http://dx.doi.org/10.1021/ac062160k.
[71] Seybold PG, Gouterman M, Callis J. Calorimetric, photometric and lifetime determinations of fluorescence yields of fluorescein dyes. Photochem Photobiol 1969;9:229–42.
[72] Förster T. Zwischenmolekulare Energiewanderung und Fluoreszenz. Ann Phys 1948;437:55–75. http://dx.doi.org/10.1002/andp.19484370105.
[73] Marcus RA, Sutin N. Electron transfers in chemistry and biology. Biochim Biophys Acta 1985;811:265–322. http://dx.doi.org/10.1016/0304-4173(85)90014-X.
[74] Levich VG, Dogonadze RR. Theory of nonradiation electron transitions from ion to ion solns. Dokl Akad Nauk SSSR 1959;124:123–6.
[75] Kotelnikov AI. The analysis of experimental data on electron conductivity of globular proteins. Biofizika 1993;38:228–32.
[76] Moser CC, Keske JM, Warncke K, Farid RS, Dutton PL. Nature of biological electron transfer. Nature 1992;355:796–802. http://dx.doi.org/10.1038/355796a0.
[77] Kotelnikov AI, Vogel VR, Pastuchov AV, Voskoboinikov VL, Medvedev ES. Coupling of electron transfer and protein dynamics. In: Canters GV, Vijgenboom E, editors. Biol. Electron Transf. Chain. Genet. Compos. Mode Oper. NATO ASI Ser. Ser. C Math. Phys. Sci., Dordrecht/Boston/London. The Netherlands: Kluwer Academic Publishers; 1998. p. 29–49.
[78] Gray HB, Winkler JR. Heme protein dynamics: electron tunneling and redox triggered folding. Porphyr. Handb. Elsevier; 2003. p. 51–73. http://dx.doi.org/10.1016/B978-0-08-092385-7.50008-2.
[79] Wang F, Cui X, Lou Z, Zhao J, Bao M, Li X. Switching of the triplet excited state of rhodamine-C_{60} dyads. Chem Commun Camb 2014;50:15627–30. http://dx.doi.org/10.1039/c4cc07603f.
[80] Poletaeva DA, Kotel'nikova RA, Mischenko DV, Rybkin AY, Smolina AV, Faingol'd II , et al. Estimation of membrane activity of water-soluble polysubstituted fullerene derivatives by luminescence methods. Nanotechnol. Russ 2012;7:302–7. http://dx.doi.org/10.1134/S1995078012030135.